Journal of Pharmaceutical and Biomedical Analysis 177 (2020) 112845

Contents lists available at ScienceDirect

Journal of Pharmaceutical and Biomedical Analysis

journal homepage: www.elsevier.com/locate/jpba

Quantifying protein aggregation kinetics using electrospray differential mobility analysis

Kaleb J. Duelge[a,b,*], Jeremie Parot[a], Vincent A. Hackley[a], Michael R. Zachariah[a,b,c]

[a] National Institute of Standards and Technology, 100 Bureau Dr., MS 8520, Gaithersburg, MD, 20899-8520, United States
[b] University of Maryland, College Park, United States
[c] University of California, 900 University Ave., Riverside, CA, 92521, United States

ARTICLE INFO

Article history:
Received 11 July 2019
Received in revised form 27 August 2019
Accepted 28 August 2019
Available online 30 August 2019

Keywords:
Differential mobility
Protein aggregation
Aggregation kinetics

ABSTRACT

Protein aggregation is a critical concern in bioprocessing, where its presence can result in serious adverse interactions in clinical end-use applications. In this study, an aerosol-based technique, electrospray differential mobility analysis (ES-DMA), was used to quantify thermally-induced protein aggregation kinetics for bovine serum albumin (BSA) and α-chymotrypsinogen A (α-chymo), employing a new methodology to modify the solution for compatibility with the electrospray process. Results are compared orthogonally with asymmetrical-flow field-flow fractionation (AF4), a hydrodynamic separation technique with UV detection. Measurements were conducted over a range of protein concentrations and temperatures. Both techniques successfully resolved the protein monomer and dimer populations, allowing quantification of monomer loss. BSA and α-chymo exhibited second and first order kinetics, respectively, confirming different limiting steps for the two species. The Arrhenius equation yielded activation energies for BSA of (240 ± 20) kJ mol^{-1} and (190 ± 10) kJ mol^{-1} by ES-DMA and AF4, respectively. The rates determined by ES-DMA were equal to or slightly faster than those measured by AF4, so instrumental differences were analyzed to identify potential sources of bias. An important factor may be the applicable concentration range for each method; notably, AF4 operates at the mg mL^{-1} level, while ES-DMA is sensitive at μg mL^{-1} and therefore requires much smaller samples for analysis (typically several μL are injected). The limitations of each method are detailed in the discussion and demonstrate the importance of orthogonal measurement strategies for the analysis of protein kinetics. ES-DMA provides a potentially useful alternative to size exclusion chromatography to screen the stability of formulation conditions for protein therapeutics; neither ES-DMA nor AF4 rely on column interactions for separation.

1. Introduction

Aggregation is an important concern in the protein therapeutics industry. Aggregation can reduce the dose of active drug, resulting in variable efficacy. More importantly, aggregates can trigger a severe immune response including anaphylaxis and in some cases death. As a result, protein products must be thoroughly screened for aggregates throughout the production process. The most basic regulatory requirement for injections is the United States Pharmacopeia Reference Standard 788, which sets particle-per-container specifications as detected by light obscuration. This standard is used by quality control personnel to screen products prior to distribution. Ideally, aggregate formation is prevented much earlier in the product cycle. Aggregation kinetics are measured extensively during formulation and in the initial stages of production, and the buffer, pH and excipients are optimized to produce a stable formulation. Different stress conditions are applied, including shaking, stirring, heating and changing pH to mimic situations that can be encountered during the manufacturing process. The challenge, however, is to verifiably measure aggregation at all potential growth stages, from both a process control standpoint as well as a view to the science of protein aggregation. Many measurement approaches have been adopted to evaluate aggregates and aggregation rates, including light scattering, sodium dodecyl sulfate polyacrylamide gel electrophoresis, analytical ultracentrifugation, fluorescence, absorbance, calorimetry and field-flow fractionation [1]. The most commonly used technique in industry currently is size exclusion chromatography (SEC) [2], although no single technique has been established that has satisfied all characterization needs.

* Corresponding author at: National Institute of Standards and Technology, 100 Bureau Dr., MS 8520, Gaithersburg, MD, 20899-8520, United States
E-mail addresses: kaleb.duelge@nist.gov (K.J. Duelge), vince.hackley@nist.gov (V.A. Hackley), mrz@engr.ucr.edu (M.R. Zachariah).

https://doi.org/10.1016/j.jpba.2019.112845
0731-7085/

Absolute aggregation kinetics data are fraught with a range of interference effects including adsorption [3], membrane interaction [4], aggregate disruption [5], dilution effects [6], and convolution [7]. Thus, there is a considerable need for assessing methods in terms of absolute and relative accuracy and precision.

In the present work, a lesser known but rapid, high-resolution aerosol-based technique, electrospray differential mobility analysis (ES-DMA, see Fig. 1), is applied to quantify the thermally induced aggregation kinetics of two selected proteins in an extensive and systematic study. This work builds on two previous studies conducted at the National Institute of Standards and Technology. Pease et al. [8] showed that ES-DMA can resolve and accurately size IgG aggregate oligomers prepared by pH-induced unfolding and chemical-induced crosslinking. Subsequently, Guha et al. [9] compared ES-DMA with the "gold standard," SEC, for thermal aggregation of IgG. The latter study examined oligomer size and concentration, while also determining and comparing aggregation rates between the two techniques (where aggregation was carried out in an ammonium acetate buffer to support the electrospray process). Ammonium acetate is an ideal and commonly used electrolyte for ES-DMA due to its volatility; nonvolatile salts will interfere with the ES-DMA analysis and alter the size of classified aggregates. However, ammonium acetate is not relevant for the measurement of protein aggregation, and can itself induce unfolding leading to aggregation [10]. In building on these earlier studies, this new method determines protein aggregation rates using the monomer loss approach combined with ES-DMA. In the current work, aggregation was conducted in common protein formulation buffers followed by post-reaction dilution into ammonium acetate. The aggregation rates are therefore determined by the buffer used during thermal treatment. Using this method, protein aggregation kinetics are quantified under a range of conditions and demonstrate the full capacity for application of ES-DMA as an alternative technique relevant to protein drug development and manufacturing. To cross-validate this method and demonstrate that the measured kinetics are reliable, a direct orthogonal comparison is provided between ES-DMA and asymmetrical flow field-flow fractionation (AF4), a liquid-based method that separates particles according to their diffusivity (hydrodynamic size) [11]. AF4 was selected in this case over SEC so that protein samples could be analyzed in the formulation buffers without any change in buffer composition or ionic strength. A more detailed description of AF4 is provided in the supplemental material.

To facilitate this investigation, two well characterized and widely available model proteins were selected, namely bovine serum albumin (BSA) and α-chymotrypsinogen A (α-chymo). Both proteins are stable in solution at room temperature for at least one day and have been previously studied in kinetic experiments [1,12]. BSA is a 66.3 kDa globular protein with an isoelectric point (pI) of 4.8 and a hydrodynamic diameter of 7.0 nm [13]. α-chymo is a 25.7 kDa globular protein with a pI of 9.2 and a hydrodynamic diameter of 4.4 nm [14]. Commercial α-chymo contains a small amount of chymotrypsin that can cleave peptide bonds above pH 5, so experiments were conducted at pH 3.5 [15]. Neither protein is used as a therapeutic, but human serum albumin is used as a carrier for paclitaxel in Abraxane, an approved treatment for metastatic cancer. On the other hand, α-chymo is the inactive precursor to chymotrypsin, a proteolytic enzyme produced in the pancreas.

2. Materials and methods

BSA (>96%), α-chymo (essentially salt-free, lyophilized powder), sodium phosphate dibasic (>99%), citric acid (99.5%), ammonium acetate (>99.99%) and sodium citrate dihydrate (>99.9%) were purchased from Sigma Aldrich (St. Louis, MO, USA).[5] Sodium phosphate monobasic (99%) was purchased from Alfa Aesar (Haverhill, MA, USA). Solutions were prepared using 18.2 MΩ cm deionized water (Model 2121AL, Aqua Solutions, Jasper, GA, USA). BSA solutions were prepared by dissolving lyophilized BSA in 0.1 mol L^{-1} phosphate buffer at pH 7.0. α-chymo solutions were prepared by dissolving lyophilized α-chymo in 0.01 mol L^{-1} citrate buffer at pH 3.5 and were filtered before use (0.2 μm, Whatman, Maidstone, UK). Protein concentration was determined spectroscopically at 280 nm using published 1% mass extinction coefficients: 6.58 for BSA [13] and 19.7 for α-chymo [16]. Protein solutions were diluted to the working concentration and volume, then aliquoted to protein lo-bind microcentrifuge tubes (Eppendorf, Hamburg, Germany). For temperature studies, protein samples were heated in a water bath (Model WD05V11B, VWR, Radnor, PA, USA) and quenched in an ice bath at the designated time point. Each sample was analyzed by both AF4 and ES-DMA. Aliquots for ES-DMA were diluted to 0.009 mg mL^{-1} in 0.4 mol L^{-1} ammonium acetate at pH 7.0 or 0.02 mol L^{-1} ammonium acetate at pH 3.5, for BSA and α-chymo, respectively. Ammonium acetate provides sufficient conductivity for the ES process and leaves no aerosol residue. Aliquots for AF4 were injected into the instrument without modification.

The customized ES-DMA system used in this study, similar to those reported by others [17], consists of three principal components: the ES (Model 3480, TSI, Shoreview, MN, USA), differential mobility electrode column (Model 3085, TSI), and condensation particle counter (Model 3776, TSI). Protein solutions were placed in the ES pressure chamber set to 26 kPa (3.7 psi) and sprayed through a 40 μm inner diameter fused silica capillary. 40 μm capillaries were used rather than the more common 25 μm capillaries to prevent clogging. Protein was electrosprayed with an air flow rate of 1 L min^{-1} and a CO_2 flow rate of 0.2 L min^{-1}. The sheath flow was 10 L min^{-1} air. The sheath flow was selected as an optimal compromise between resolution and the limit of detection. The ES voltage was set to (2–3) kV, with a resulting current of (300–1100) nA, to produce a stable Taylor cone. The electric field strength was on the order of 10^6 V m^{-1}. The resulting aerosol was neutralized by a Po-210 α-source (Model P-2042, TSI) to produce a bipolar aerosol with some positively charged, negatively charged, and uncharged particles. The differential mobility analyzer column (DMA) was operated to select positively charged protein particles. The data was collected with a step size of 0.2 nm and a step time of 5 s using a custom LabVIEW (National Instruments, Austin, TX, USA) program to control the high voltage power supply (Model 205B-10R, Spellman, Hauppauge, NY, USA). The BSA monomer yielded a mobility diameter of (6–7.6) nm with a peak at 6.8 nm. The α-chymo monomer yielded a mobility diameter of (4.2–5.6) nm with a peak at 5 nm. These sizes are consistent with previously published work using ES-DMA [8,9,18], though the sizes measured in this work were slightly larger than the uncoated monomers due to residual non-volatile buffer (sodium phosphate or sodium citrate) that coats the protein particles. The unheated protein sample was electrosprayed for one hour before data collection to minimize capillary adsorption effects. A step-ramping voltage was applied to the separation column, selecting for a series of sizes based on certain physical considerations of the instrument outlined in Eq. (1) [19],

$$\frac{d}{C_c(d)} = \frac{2neLV_{DMA}}{3\mu q_{sh}\ln(r_2/r_1)} \quad (1)$$

where d is the selected mobility diameter, C_c is the Cunningham slip correction factor, n is the number of elementary charges on the

[5] The identification of any commercial product or trade name does not imply endorsement or recommendation by the National Institute of Standards and Technology.

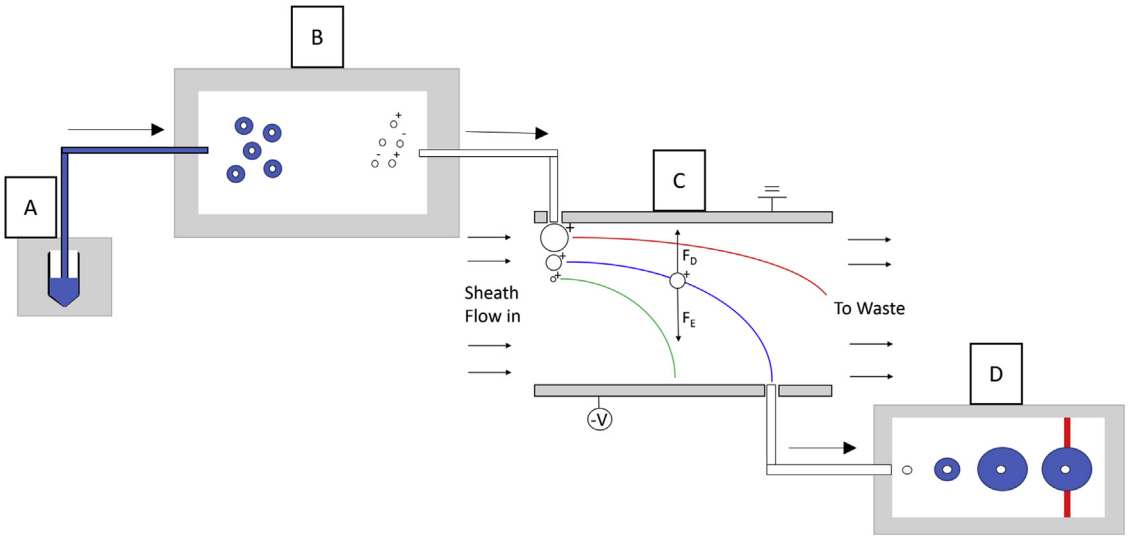

Fig. 1. ES-DMA method for the separation of nano scale particles. The protein solution is placed in a pressurized chamber and passed through a small capillary (A). The solution is electrosprayed into a neutralization chamber that yields particles with a -1, 0 or +1 charge (B). The +1 charged aerosol is separated by size in the differential mobility analyzer (C). The particles are counted optically by a condensation particle counter (D).

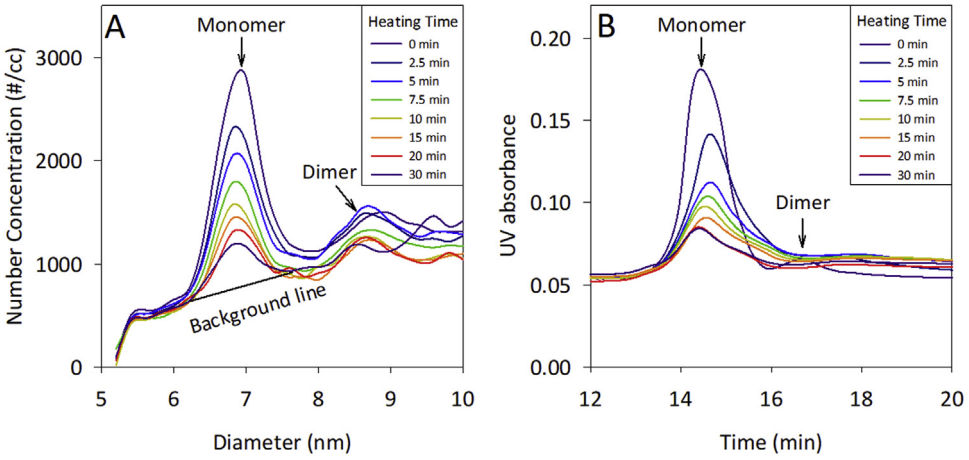

Fig. 2. (a) ES-DMA determined number-based size distribution for 1 mg mL^{-1} BSA. The monomer was determined to have a mobility diameter of (6–7.6) nm. The monomer area decreased with increasing heating time at 70 °C. The monomer area does not include the area below the background line caused by non-volatile salt. The data points are connected with a smooth line. (b) AF4 fractionation of 1 mg mL^{-1} BSA. The monomer eluted between (13 and 16) min, and the area under monomer peak decreased with increasing heating time at 70 °C. The data points are connected with a smooth line.

particle, e is the elementary charge, L is the length of the DMA, V is the voltage of the DMA, μ is the viscosity of the sheath gas, q_{sh} is the flow rate of the sheath gas, and r_2 and r_1 are the outer and inner radii of the DMA, respectively. To evaluate the number count, the raw data was corrected for charging efficiency and the DMA column transfer function [20]. When particles are neutralized by the α-emitter, a size-dependent modified Boltzmann charge distribution is applied to the population of particles. Based on the size of the particles, a known percentage will have various charges, primarily -1, 0 and +1. Only particles with a single positive charge were size selected and counted, so the number concentration was multiplied by a correction factor to account for the other charge states of the total population. For example, only 1.9% of 5 nm particles will have a single positive charge, so the measured number concentration was multiplied by 52.6 [21]. The separation resolution of the instrument is determined by the ratio of the sheath flow to the sample flow and the size of the particle [22]. The conditions of the present work have a mobility resolution of 12%. For small particles in the free molecular flow regime, the size resolution is half the mobility resolution [23], so the window (band pass) of selected particles increases from 0.18 nm at 3 nm to 0.6 nm at 10 nm. The number concentration at each step was divided by the corresponding size window.

Each time point of the kinetic plots consists of nine measurements by ES-DMA. Chauvenet's criterion was used to analyze outliers of the ES-DMA measurements [24]. The difference between the suspected outlier and the mean of the nine measurements was divided by the standard deviation and compared to a probability percentage table of a Gaussian distribution. Points with less than a 50% probability of falling within the distribution were rejected. A maximum of one measurement per time point was analyzed for rejection and no more than four total measurements were rejected from a single experiment.

For AF4 analysis, an Eclipse DualTec separation system (Wyatt Technology Inc., Santa Barbara, CA, USA) was used connected to a degasser (Gastorr TG-14, Flom Co., Ltd, Tokyo, Japan), 1260-series isocratic pump (Agilent Technologies, Santa Clara, CA, USA), 1260 ALS series autosampler (Agilent Technologies) and a 1200 series UV–vis absorbance diode array detector (Agilent Technologies). For the separation, a 145 mm short channel was equipped with a 350 μm spacer of wide width and a regenerated cellulose

Table 1
AF4 method parameters.

Flow Type	Duration (min)	Focus Flow (mL min^{-1})	Cross Flow (mL min^{-1})	Elution Flow (mL min^{-1})
Elution	1	–	–	0.5
Focus	2	2	–	–
Focus & Injection	5	2	–	–
Elution	20	–	3	0.5
Elution	5	–	–	0.5

Table 2
Rate constants for the aggregation of BSA measured by ES-DMA and AF4.

BSA Condition		Second Order Rate Constant (L mol^{-1} s^{-1})	
Concentration (mg mL^{-1})	Temperature (°C)	ES-DMA	AF4
1	75	130 ± 10	130 ± 10
1	70	120 ± 20	94 ± 10
1	65	32 ± 1	23 ± 1
1	60	9 ± 1	9.1 ± 0.1
5	70	110 ± 10	75 ± 1
1.5	70	94 ± 3	73 ± 2
1	70	120 ± 20	94 ± 10

Table 3
Rate constants for the aggregation of α-chymo measured by ES-DMA and AF4.

α-chymo Condition		First Order Rate Constant (1E-5 s^{-1})	
Concentration (mg mL^{-1})	Temperature (°C)	ES-DMA	AF4
1	62.5	160 ± 10	150 ± 10
1	60	110 ± 10	110 ± 10
1	57.5	52 ± 1	45 ± 2
1	55	9.7 ± 0.9	8.8 ± 0.5
2	60	300 ± 10	340 ± 10
1.5	60	200 ± 10	180 ± 10
1	60	110 ± 10	110 ± 10

membrane with a 10 kDa cutoff. The UV signal was detected at 280 nm. The elution, injection and cross flow rates were fixed at 0.5 mL min^{-1}, 0.2 mL min^{-1} and 3 mL min^{-1} respectively. The injection volume was varied, based on the sample concentration, to inject (50–60) μg of protein. The focus flow and cross flow rates, during the relaxation and the elution, were optimized as a function of the size distribution of the sample and are summarized in Table 1. AF4 data was obtained and analyzed using OpenLab (Agilent Technologies) and Astra 6.1.4.25 software (Wyatt Technology). The monomer peak was manually defined and integrated with the absorbance signal between (13 and 16) min elution time for BSA and (10.5 and 14) min for α-chymo.

3. Results and discussion

The monomer and the dimer were distinguishable using both techniques, and thus the temporal, relative monomer decline was used as the primary observation of aggregation. This separation is important because it indicates that any larger species will not coelute with the monomer. The decline of the isolated monomer determines the measured rate of aggregation. Fig. 2a shows the ES-DMA measured number-based size distribution of BSA as a function of heating time, indicating the BSA monomer had a mobility diameter of (6 to 7.6) nm. Fig. 2b shows the AF4 measured fractogram of BSA as a function of heating time, indicating the BSA monomer elutes between (13 and 16) min. To correct for background signal from residual non-volatile buffer a baseline correction was applied for ES-DMA as shown in the figure. The monomer peak area was then determined by subtracting the total area under the monomer peak by the area of the background for each time point and normalized to the unheated sample.

As expected, the rate of aggregation for both proteins increased at higher concentration and temperature. These results are summarized in Fig. 3 as the mean of three independent samples. For AF4, each sample was analyzed once, while for ES-DMA each sample was analyzed three times under repeatability conditions. For AF4, the error bars indicate one standard deviation of the three measurements. For ES-DMA, the three repeatability measurements were averaged for each sample and the error bars indicate one standard deviation of the three means. The normalized monomer peak area was multiplied by the concentration of the unheated solution and divided by the molar mass to convert to molarity. The goodness-of-fit (using R^2) for the linear regression of molarity vs. time, ln (molarity) vs. time, and (molarity)$^{-1}$ vs. time was then used to assess if the aggregation was best represented as zero, first or second order, respectively.

Results included in the supplementary material show that BSA exhibits second order behavior and α-chymo is most consistent with a first order monomer decay. This suggests BSA aggregation is limited by monomer-monomer collisions, while α-chymo is limited by monomer thermal unfolding or monomer addition to aggregates. When elevated temperature is used as a stress, aggregation is minimal below the melting temperature of a protein. This indicates that the unfolding of the protein is critical in thermal aggregation. A first order kinetic rate suggests a single protein population is the limiting reactant for aggregation to occur. The aggregation rate for α-chymo varies with initial protein concentration. This suggests that the monomer interacts with another species (e.g., an aggregate) that is an important co-determinant of the rate of aggregation. Also, the unfolding rate of α-chymo is much faster than the aggregation rate [25]. This suggests that α-chymo aggregation is limited by monomer addition rather than unfolding. For second order kinetics, the protein molecules are also unfolded,

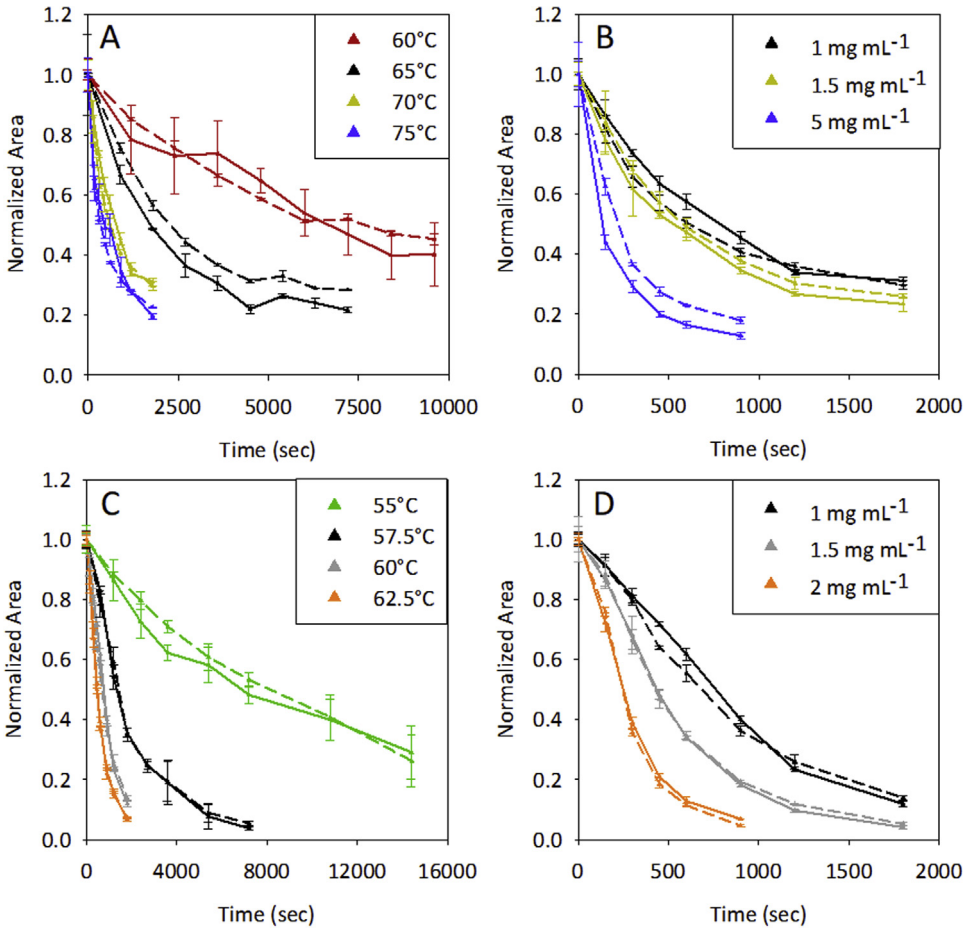

Fig. 3. Normalized protein monomer peak area as a function of time and incubation temperature or incubation concentration measured by ES-DMA (solid lines) and AF4 (dashed lines). Lines are guides only. (a) 1 mg mL^{-1} BSA incubated at different temperatures. (b) BSA heated at 70 °C and incubated at different concentrations. (c) 1 mg mL^{-1} α-chymo incubated at different temperatures. (d) α-chymo heated at 60 °C and incubated at different concentrations.

but the collision between two monomers is the limiting step. The ln (molarity) vs. time and (molarity)$^{-1}$ vs. time data was fit with a weighted least squares regression to account for differences in the standard deviation at various times and to determine the most representative slope and uncertainty for a linear fit [24].

$$y = A + Bx \tag{2}$$

$$B = \frac{\Sigma w \Sigma wxy - \Sigma wx \Sigma wy}{\Sigma w \Sigma wx^2 - (\Sigma wx)^2} \tag{3}$$

$$\sigma_B = \sqrt{\frac{\Sigma w}{\Sigma w \Sigma wx^2 - (\Sigma wx)^2}} \tag{4}$$

Where A is the intercept, B is the slope, σ_B is the uncertainty of the slope and $w_i = \sigma_i{}^{-2}$. The rate constants are compiled in Tables 2 and 3. Note that the BSA rate constant for 70 °C and 1 mg mL^{-1} is the mean (with standard deviation) of three experiments performed on three separate days: (120 ± 20) L mol^{-1} s^{-1} and (94 ± 10) L mol^{-1} s^{-1}, by ES-DMA and AF4, respectively. This is significantly higher than (62 ± 2) L mol^{-1} s^{-1} reported previously using AF4 [1]. The difference might be attributable to BSA batch variations. Also, the rate constant obtained here for 1 mg mL^{-1} α-chymo heated at 60 °C was (110 ± 10) s^{-1} by ES-DMA and AF4. This is close to 93 s^{-1} reported previously using size exclusion chromatography [12]. Li et al. reported a half-life of about 14 min, compared with about 11 min determined in the present study using both ES-DMA and AF4. In this work, the rate constants increased with increasing temperature. The rate constant for α-chymo increased with increasing concentration, while the rate constant for BSA decreased or remained the same with increasing concentration.

The activation energy was determined using an Arrhenius plot, with (absolute temperature)$^{-1}$ vs. ln (rate constant) as shown in Fig. 4. The non-linear plots indicate that the studied proteins are non-Arrhenius in the given temperature range. This indicates a change in the rate determining step at different temperatures. The change in the aggregation rate decreased at higher temperatures. The low temperature region for BSA, from (60 to 70) °C was linear and was used to calculate the activation energy. The obtained value contains information regarding the thermal unfolding of the protein and the collision required to produce a dimer. The energies reported here for BSA, (240 ± 20) kJ mol^{-1} and (190 ± 10) kJ mol^{-1} by ES-DMA and AF4 respectively, are of similar magnitude to those reported in the literature for other proteins: (350 to 550) kJ mol^{-1} [2,26,27].

The rates measured by ES-DMA were generally equal to or slightly faster than those by AF4. Many aspects of the measurement techniques could result in a faster measured rate. For example, ES-DMA requires a dilution and buffer exchange, uses a fused silica capillary and can cause droplet-induced aggregation during the ES process. ES-DMA requires a volatile buffer and dilute protein solution for the ES, so the protein samples were diluted into ammonium acetate immediately before analysis. Non-volatile buffer components can lead to peak broadening, an elevated baseline and a shift in detected diameter values. An undetermined maximum non-volatile buffer concentration exists (specific to the given protein and conditions) that will prevent protein detection even with dilu-

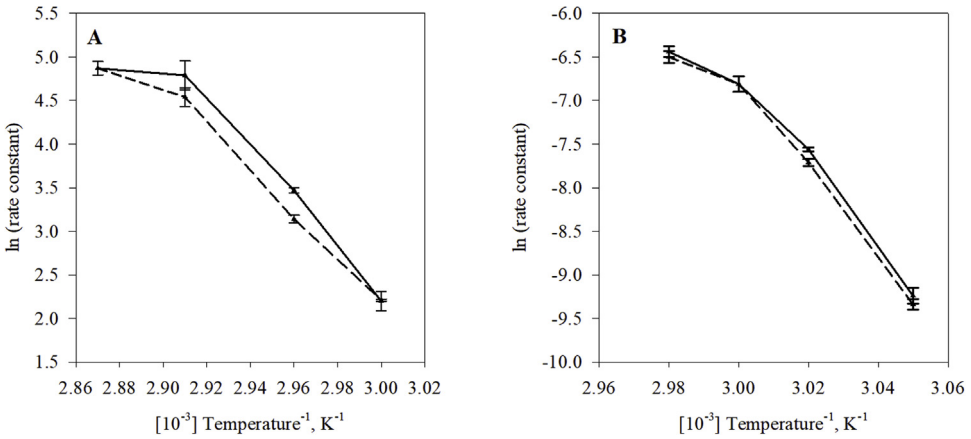

Fig. 4. Arrhenius plots of BSA and α-chymo determined by ES-DMA (solid lines) and AF4 (dashed lines) rate measurements. Lines are guides only. (a) Arrhenius plot of BSA from (60 to 75) °C. The linear region from (0.00291 to 0.003) K^{-1} was used to determine the activation energy. (b) Arrhenius plot of α-chymo from (55 to 62.5) °C. The non-linear behavior indicates different rate limiting behavior at different temperatures.

tion in ammonium acetate. BSA was in a higher concentration of non-volatile buffer (0.1 mol L^{-1} phosphate buffer) than α-chymo, so a higher ionic strength of ammonium acetate was required. The higher ionic strength produces smaller droplets in the ES process [28]. These smaller droplets contain less of the non-volatile salt and therefore mask the protein to a lesser degree. An alternative buffer exchange method, centrifuge filtration, showed no significant difference in the rates measured by ES-DMA (results not shown). The observed difference between ES-DMA and AF4 data is similar for both BSA and α-chymo, which suggests that the ionic strength of the dilution buffer does not have a significant effect on the kinetics. Another possible contribution to the differences in the observed rates could be due to proteins adhering to the fused silica capillary [18]. Protein loss to the capillary surface would be convoluted with aggregated protein, as both result in the loss of monomer. This effect was minimized by equilibrating the capillary with the unheated protein sample for one hour prior to data collection. Future work could investigate capillary surface modification to reduce protein adsorption and limit the required equilibration time. Finally, the ES process can cause aggregation if two protein monomers are contained within a single droplet (i.e., coincidence) [29]. This artifact would be detected as a protein dimer, because the two monomers merge as the droplet evaporates. This could cause an apparent monomer loss if the ES droplet size varied with time. This effect was minimized by spraying a stable Taylor cone and diluting the protein sufficiently. Overall, there are many potential sample and instrumental causes of the observed rate differences, though many have been accounted for in the current work. An extensive cause and effect analysis was beyond the scope of the present work.

AF4 creates less concern for instrumental influences on the measured aggregation rate. Only the focus step, the concentrating of injected protein on the surface of the membrane prior to separation, is likely to cause artifacts. This process could potentially result in protein adsorption or aggregation. Since the membrane is negatively charged, positively charged particles tend to stick to its surface. It was observed that positively charged α-chymo absorbed significantly onto the regenerated cellulose membrane, and several injections were required to reach a steady state (i.e., membrane saturation). In addition, a loss in separation efficiency was observed after many injections and separations. The initial smooth, Gaussian distribution of the monomer devolved into a tailed elution of protein at longer retention times, likely due to protein-protein attraction at the membrane surface. A new membrane was used after every two experiments as the monomer peak began to shift and distort. This will likely be a problem for any aggregation measured below the pI of the protein. An alternative means to deal with this is to treat the membrane with a cationic surfactant to electrostatically repel the protein [30]. This strategy was not pursued as it adds further uncertainty due to protein-surfactant interactions.

4. Conclusions

This study investigated the application of an aerosol-based technique, electrospray differential mobility analysis (ES-DMA), as an alternative method to quantify protein aggregation kinetics. Building on two previous studies, the method described here is more generally applicable, as it can be used to assess protein aggregation in any buffer. Additionally, ES-DMA was directly cross-validated with an orthogonal liquid-based separation technique, asymmetrical-flow field-flow fractionation (AF4). Consistent rate constants were obtained between the two methods; second order for bovine serum albumin (BSA) and first order for α-chymotrypsinogen A (α-chymo). The two techniques have different advantages that lend themselves to specific applications. AF4 yielded more consistent data, as the standard deviation of the monomer peak area was (1–5) %, compared to (5–10) % for ES-DMA. However, the ES-DMA method is much faster in practice; the AF4 method required 34 min for analysis, while the ES-DMA analysis was complete in just 4 min after a single, 1 h capillary equilibration, a significant advantage for thorough characterization of various aggregation conditions. As a result, this study accommodated three times as many measurement results by ES-DMA compared with AF4. Also, AF4 uses substantial amounts of mobile phase during separation; roughly three liters of buffer were required per experiment. In contrast, ES-DMA uses a gas phase to separate the particles, resulting in minimal waste. Finally, approximately 100 μg of protein was injected per measurement for AF4, compared with 100 ng for ES-DMA. In this respect, AF4 is comparable to SEC, the current gold standard method in industry. ES-DMA has significant potential for screening valuable proteins in limited supply, as an entire kinetics study requires only 2 mg (limited primarily by buffer evaporation during heating). However, ES-DMA has significant limitations, including dilution, buffer exchange, buffer volatility, capillary adsorption and droplet aggregation that, while controlled to the extent possible in this study, could be improved in future developments. Future work could also include hyphenation of ES-DMA with mass spectrometry to determine concurrent kinetic and structural information, for instance whether there is a specific aggregation-prone region and how this might change with

different applied stresses, and further optimization of the electrospray process for proteins to reduce protein loss artifacts and further reduce overall analysis time.

Declaration of Competing Interest

The authors declare that they have no conflict of interest.

Acknowledgement

KJD was supported by the National Institute of Standards and Technology [grant number 70NANB17H057].

Appendix A. Supplementary data

Supplementary material related to this article can be found, in the online version, at doi:https://doi.org/10.1016/j.jpba.2019.112845.

References

[1] V.A. Borzova, et al., A change in the aggregation pathway of bovine serum albumin in the presence of arginine and its derivatives, Sci. Rep. 7 (2017) 12.
[2] M. Weijers, et al., Heat-induced denaturation and aggregation of ovalbumin at neutral pH described by irreversible first-order kinetics, Protein Sci. 12 (12) (2003) 2693–2703.
[3] D. Ejima, et al., Arginine as an effective additive in gel permeation chromatography, J. Chromatogr. A 1094 (1-2) (2005) 49–55.
[4] R.R. Burgess, A brief practical review of size exclusion chromatography: rules of thumb, limitations, and troubleshooting, Protein Expr. Purif. 150 (2018) 81–85.
[5] D.K. Clodfelter, M.A. Nussbaum, J. Reilly, Comparison of free solution capillary electrophoresis and size exclusion chromatography for quantitating non-covalent aggregation of an acylated peptide, J. Pharm. Biomed. Anal. 19 (5) (1999) 763–775.
[6] J.M.R. Moore, T.W. Patapoff, M.E.M. Cromwell, Kinetics and thermodynamics of dimer formation and dissociation for a recombinant humanized monoclonal antibody to vascular endothelial growth factor, Biochemistry 38 (42) (1999) 13960–13967.
[7] J.P. Gabrielson, et al., Common excipients impair detection of protein aggregates during sedimentation velocity analytical ultracentrifugation, J. Pharm. Sci. 98 (1) (2009) 50–62.
[8] L.F. Pease, et al., Determination of protein aggregation with differential mobility analysis: application to IgG antibody, Biotechnol. Bioeng. 101 (6) (2008) 1214–1222.
[9] S. Guha, et al., Electrospray-differential mobility analysis as an orthogonal tool to size-exclusion chromatography for characterization of protein aggregates, J. Pharm. Sci. 101 (6) (2012) 1985–1994.
[10] F. Hofmeister, Zur Lehre von der Wirkung der Salze, Arch. Exp. Pathol. Pharmakol. 24 (1888) 247–260.
[11] K.G. Wahlund, J.C. Giddings, Properties of an asymmetrical flow field-flow fractionation channel having one permeable wall, Anal. Chem. 59 (9) (1987) 1332–1339.
[12] Y. Li, B.A. Ogunnaike, C.I. Roberts, Multi-variate approach to global protein aggregation behavior and kinetics: effects of pH, NaCl, and temperature for alpha-chymotrypsinogen A, J. Pharm. Sci. 99 (2) (2010) 645–662.
[13] S.C. Gill, P.H. Vonhippel, Calculation of protein extinction coefficients from amino acid sequence data, Anal. Biochem. 182 (2) (1989) 319–326.
[14] B.S. Hartley, Amino-acid sequence of bovine chymotrypsinogen-A, Nature 201 (492) (1964), p. 1284-&.
[15] O.D. Velev, E.W. Kaler, A.M. Lenhoff, Protein interactions in solution characterized by light and neutron scattering: comparison of lysozyme and chymotrypsinogen, Biophys. J. 75 (6) (1998) 2682–2697.
[16] M, S, Peptides and proteins, in: S. H (Ed.), Handbook of Biochemistry, The Chemical Rubber Co., Cleveland, OH, 1970, pp. 71–98.
[17] S.L. Kaufman, et al., Macromolecule analysis based on electrophoretic mobility in air: globular proteins, Anal. Chem. 68 (11) (1996) 1895–1904.
[18] S. Guha, et al., Protein adsorption-desorption on electrospray capillary walls - no influence on aggregate distribution, J. Colloid Interface Sci. 377 (2012) 476–484.
[19] TSI, Series 3080 Electrostatic Classifiers Operation and Service Manual, 2009.
[20] Y. Kousaka, K. Okuyama, M. Adachi, Determination of particle size distribution of ultra-fine aerosols using a differential mobility analyzer, Aerosol Sci. Technol. 4 (2) (1985) 209–225.
[21] A. Wiedensohler, An approximation of the bipolar charge distribution for particles in the submicron size range, J. Aerosol Sci. 19 (3) (1988) 387–389.
[22] E.O. Knutson, K.T.W, Aerosol classification by electric mobility: apparatus, theory, and applications, J. Aerosol Sci. 6 (6) (1975) 443–451.
[23] G.W. Mulholland, et al., Measurement of 100 nm and 60 nm particle standards by differential mobility analysis, J. Res. Inst. Stand. Technol. 111 (4) (2006) 257–312.
[24] J.R. Taylor, An Introduction to Error Analysis, 2nd ed., University Science Books, Sausalito, CA, 1997.
[25] J.M. Andrews, C.J. Roberts, Non-native aggregation of alpha-chymotrypsinogen occurs through nucleation and growth with competing nucleus sizes and negative activation energies, Biochemistry 46 (25) (2007) 7558–7571.
[26] V. Kayser, et al., Glycosylation influences on the aggregation propensity of therapeutic monoclonal antibodies, Biotechnol. J. 6 (1) (2011) 38–44.
[27] T. Spiegel, Whey protein aggregation under shear conditions – effects of lactose and heating temperature on aggregate size and structure, Int. J. Food Sci. Technol. 34 (5-6) (1999) 523–531.
[28] D.R. Chen, D.Y.H. Pui, S.L. Kaufman, Electrospraying of conducting liquids for monodisperse aerosol generation in the 4 nm to 1.8 μm diameter range, J. Aerosol Sci. 26 (6) (1995) 963–977.
[29] M.D. Li, et al., Quantification and compensation of nonspecific analyte aggregation in electrospray sampling, Aerosol Sci. Technol. 45 (7) (2011) 849–860.
[30] N. Bendixen, et al., Membrane-particle interactions in an asymmetric flow field flow fractionation channel studied with titanium dioxide nanoparticles, J. Chromatogr. A 1334 (2014) 92–100.